https://ntrs.nasa.gov/search.jsp?R=19770007007 2020-03-22T12:21:52+00:00Z

General Disclaimer

One or more of the Following Statements may affect this Document

- This document has been reproduced from the best copy furnished by the organizational source. It is being released in the interest of making available as much information as possible.

- This document may contain data, which exceeds the sheet parameters. It was furnished in this condition by the organizational source and is the best copy available.

- This document may contain tone-on-tone or color graphs, charts and/or pictures, which have been reproduced in black and white.

- This document is paginated as submitted by the original source.

- Portions of this document are not fully legible due to the historical nature of some of the material. However, it is the best reproduction available from the original submission.

Produced by the NASA Center for Aerospace Information (CASI)

NSG-7101

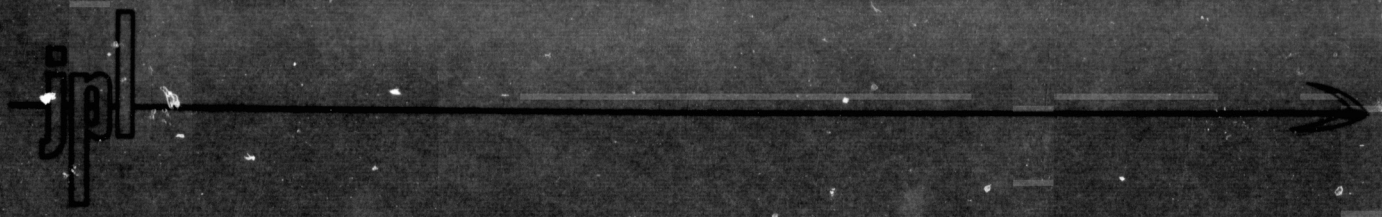

(NASA-CR-149316) EFFECTS OF STREAM-ASSOCIATED FLUCTUATIONS UPON THE RADIAL VARIATION OF AVERAGE SOLAR-WIND PARAMETERS (Jet Propulsion Lab.) 52 p HC A04/MF A01 CSCL 03B G3/92

N77-13950

Unclas
57930

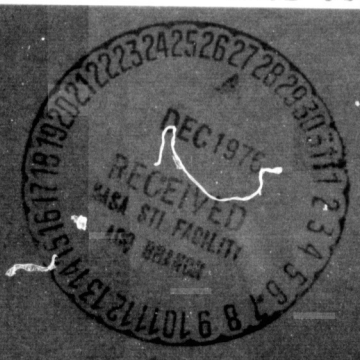

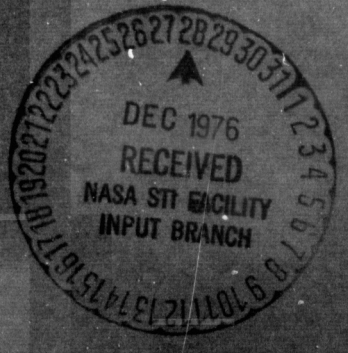

JET PROPULSION LABORATORY
CALIFORNIA INSTITUTE OF TECHNOLOGY
PASADENA, CALIFORNIA

EFFECTS OF STREAM-ASSOCIATED FLUCTUATIONS UPON THE RADIAL VARIATION OF AVERAGE SOLAR-WIND PARAMETERS

by

Bruce E. Goldstein*

J. R. Jokipii†

*Jet Propulsion Laboratory, Pasadena, California 91103
Temporarily at National Aeronautics and Space Administration
Code SL, Washington, DC 20546 until August, 1977

†Department of Planetary Sciences, Department of Astronomy
Unviersity of Arizona, Tucson, Arizona 85721

ABSTRACT

The effects of nonlinear fluctuations due to solar-wind streams upon radial gradients of average solar-wind parameters are computed, using a numerical MHD model for both spherically symmetric-time dependent and corotating equatorial-flow approximations. We find significant effects of correlations between fluctuations upon the gradients of azimuthal magnetic field, radial velocity, density and azimuthal velocity. The averages of V_r and r^2n both decrease with increasing radial distance (0 to 30 km/sec, 5 to 10% by 6 AU) while mass flux is conserved. The cross-variance between V_r and r^2n increases with radial distance from negative values to positive values at distances greater than 3.5 AU. The average azimuthal velocity decreases, and at distances greater than 4 AU may be opposite to the solar rotation; $\langle V_\phi \rangle$ of from 0.2 to -1.7 km/sec at 6 AU is predicted. Between 400 to 900 solar radii stream interactions have transferred the major portion of the angular-momentum flux to the magnetic field; at even greater distances the plasma again carries the bulk of the angular-momentum flux. The average azimuthal component of the magnetic field may decrease as much as 10% faster than the Archimedean spiral out to 6 AU due to stream interactions, but this result is dependent upon inner boundary conditions.

1. INTRODUCTION

Recent observations carried out over large ranges of heliocentric distances with deep space probes have determined the radial gradients of various solar-wind parameters (velocity, magnetic field, etc.). Theoretical analyses of the radial variations have conventionally been carried out by attempting to construct steady-state fluid dynamical models which reproduce the time averaged parameters. However, this approach neglects possible effects of correlations between large fluctuations in the parameters; the observed, large, non-linear fluctuations can be correlated to change the average properties of the solar wind (Siscoe, 1970; Jokipii, 1975, 1976) in a way that cannot be reproduced in a non-fluctuating model. For example, Schubert and Coleman (1968) have suggested that MHD fast waves may carry a substantial portion of the solar wind angular momentum flux, Pizzo et al. (1973) and Neugebauer (1976) have shown that fluctuations will alter the expected relation between temperature and velocity in the solar wind, and Jokipii (1975) has suggested fluctuations as a possible explanation for the faster than 1/r decrease in the azimuthal interplanetary magnetic field (but Parker and Jokipii (1976) show that for Pioneer 10 data inclusion of the variation of the average solar wind velocity considerably improves

agreement with the Parker spiral field).

In the theoretical analysis (Siscoe, 1970; Jokipii, 1975, 1976), the relevant fluctuating quantities which were shown to affect the mean were the correlations between fluctuations, and their radial variations. The magnitudes of these correlations were left either to direct measurements or to theoretical calculations based on solar-wind models. It is the purpose of this paper to present the results of detailed numerical calculations intended to reveal the existence and possible magnitude of the effects of fluctuations on the averages of selected solar-wind parameters. Since variations and correlations associated with stream structure at periods greater than one day are observed to dominate the fluctuations in the solar wind (Goldstein and Siscoe, 1972), the calculations presented here concentrate on the effects of stream-related phenomena on the radial dependence of average solar-wind parameters.

The organization of this paper is as follows: In the next section the model and computational techniques are described in detail. Section 3 discusses effects of stream structure upon the radial gradient of the density-velocity correlation in the solar wind, and the consequences for deceleration of the solar wind and estimates of solar wind heating. Section 4 continues this discussion in the context of angular-momentum transport and the average azimuthal velocity; it is demonstrated that at distances of 4 AU and beyond the average azimuthal velocity may be in the direction

opposite to the solar rotation. In section 5 the variation of B_ϕ with radius is investigated; for certain sets of inner boundary conditions (not the most realistic) the effect of stream variations is to distort the average of B_ϕ from the Archimedean spiral. In section 6 we summarize our results and discuss the observational consequences.

2. EQUATIONS, BOUNDARY CONDITIONS, AND NUMERICAL SOLUTIONS

Our starting point is the equations of motion for an MHD fluid written in conservation-law form (Rossi and Olbert, 1970). Ignoring displacement currents and relativistic effects, these equations can be written as follows:

$$\frac{\partial \rho}{\partial t} + \nabla \cdot \rho \bar{V} = 0 \tag{1}$$

$$\frac{\partial}{\partial t} \rho \bar{V} = -\nabla \cdot [\rho \bar{V}\bar{V} + \bar{\bar{P}} - 1/\mu_0 (\bar{B}\bar{B} - \tfrac{1}{2}B^2 \delta ik)] + \rho \bar{g} \tag{2}$$

$$\frac{\partial \bar{B}}{\partial t} = \nabla \times (\bar{V} \times \bar{B}) \tag{3}$$

$$\nabla \cdot \bar{B} = 0 \tag{4}$$

$$\frac{\partial}{\partial t} (\tfrac{1}{2}\rho V^2 + \varepsilon + B^2/2\mu_0) =$$

$$-\nabla \cdot [(\tfrac{1}{2}\rho V^2 + \varepsilon)\bar{V} + \bar{\bar{P}} \cdot \bar{V} + \bar{q} + 1/\mu_0 \ \bar{B} \times (\bar{V} \times \bar{B})] + \rho \bar{g} \cdot \bar{V} \tag{5}$$

In these equations ρ is mass density, $\bar{V}$ is solar wind velocity, $\bar{B}$ is magnetic field, ε is internal energy density of the plasma, $\bar{\bar{P}}$ is the plasma pressure tensor, $\bar{q}$ is the heat flux, and $\bar{g}$ is the solar

gravitational acceleration. For the purposes of solving these equations we adopt a coordinate system in which r is radial from the sun, ϕ is the longitudinal coordinate, and θ is colatitude, and a model for plasma flow in the solar-wind equatorial plane in which $B_\theta = V_\theta = 0$ and $\frac{\partial}{\partial\theta} = 0$. The limitations of this approximation (which ignores meridional flows, i.e. $\frac{\partial V_\theta}{\partial\theta}$ and $\frac{\partial B_\phi}{\partial\theta}$ terms) are discussed in Suess and Nerney (1973). The primary effect is that flow divergence from the equatorial plane due to the r sin θ dependence of $\frac{\partial B_\phi}{\partial\theta}$ is ignored. Nerney and Suess (1975) and Winge and Coleman (1974) show that this procedure does not cause decreases of from more than 10 to 20% in B_ϕ at 5 AU due to flow divergence; somewhat larger effects may occur for V_ϕ. Rhodes and Smith (1975) have presented observational evidence for an increase in solar wind velocity with latitude; $\frac{\partial V_r}{\partial\theta}$ terms will also effect radial gradients in the equatorial plane. The effects we discuss will also occur in models that include latitudinal variations; such effects can be regarded as contributing in a somewhat independent fashion. Finally, we note that B_ϕ at high latitudes will be less than in the equatorial plane due to the sin θ dependence of rotational velocity; Suess et al. (1975) discuss theoretical models of latitudinal variations of solar wind streams.

In the equatorial-flow approximation we have

$$\frac{\partial}{\partial r}\left(r^2\rho V_r\right) = -\frac{\partial}{\partial\phi}\rho r V_\phi - \frac{\partial}{\partial t}\rho r^2 \qquad (6)$$

$$\frac{\partial}{\partial r}\left(r^2 B_r\right) = -\frac{\partial}{\partial \phi} r B_\phi \tag{7}$$

$$\frac{\partial}{\partial r} r\left(V_\phi B_r - V_r B_\phi\right) = \frac{\partial}{\partial t} r B_\phi \tag{8}$$

$$\frac{\partial}{\partial r} r^2\left[\rho V_r^2 + \tfrac{1}{2}\left(B_\phi^2 - B_r^2\right)/\mu_0 + P\right] =$$

$$\frac{\partial}{\partial \phi} r\left(B_\phi B_r/\mu_0 - \rho V_\phi V_r\right) - \frac{\partial}{\partial t} r^2 \rho V_r$$

$$+ r\left(2P + \rho\left(V_\phi^2 - G/r\right) + B_r^2/\mu_0\right) \tag{9}$$

$$\frac{\partial}{\partial r} r^3\left(\rho V_r V_\phi - B_r B_\phi/\mu_0\right) =$$

$$\frac{\partial}{\partial \phi} r^2\left(-P - \rho V_\phi^2 + \tfrac{1}{2}\left(B_\phi^2 - B_r^2\right)/\mu_0\right) - \frac{\partial}{\partial t} r^3 \rho V_\phi \tag{10}$$

$$\frac{\partial}{\partial r} r^2\left[V_r\left(\tfrac{1}{2}\rho\left(V_r^2 + V_\phi^2\right) + P + \varepsilon\right) + 1/\mu_0\, B_\phi\left(B_\phi V_r - V_\phi B_r\right)\right] = -\rho G V_r$$

$$+ \frac{\partial}{\partial \phi}\left[-r V_\phi\left(\tfrac{1}{2}\rho\left(V_r^2 + V_\phi^2\right) + \varepsilon + P\right) + r B_r\left(B_\phi V_r - V_\phi B_r\right)/\mu_0\right]$$

$$- \frac{\partial}{\partial t} r^2\left[\left(\tfrac{1}{2}\rho\left(V_r^2 + V_\phi^2\right) + \varepsilon\right) + \left(B_\phi^2 + B_r^2\right)/2\mu_0\right] \tag{11}$$

$$\frac{\partial B_r}{\partial t} = \frac{1}{r}\frac{\partial}{\partial \phi}\left(B_\phi V_r - V_\phi B_r\right) \tag{12}$$

In eq. 11 we have assumed that heat flux is zero; and we assume that pressure is a scalar, P. The effects of thermal conduction are approximated by a polytrope relation between the internal energy density and the pressure of the plasma. Thus,

$$P = P_e + P_i \tag{13}$$

$$P_e = \alpha \rho^{\gamma_e} \tag{14}$$

$$\varepsilon = \varepsilon_i + \varepsilon_e \tag{15}$$

$$\varepsilon_{e,i} = \frac{1}{\gamma_{e,i} - 1} P_{e,i} \tag{16}$$

$$\frac{d\alpha}{dt} = 0 \ . \tag{17}$$

In these equations α is a constant multiplier for the polytrope law (eq. 14) that is conserved along stream lines (eq. 17). The subscript e or i refers to the pressure, internal energy, and polytrope index of the electron or ion gas. The proton temperature is determined by conservation of energy rather than a polytrope law. This scheme was introduced for the purpose of another study; the results to be described do not depend critically upon the particular temperature law assumed.

In this study we investigate both spherically-symmetric, time-dependent solutions of the solar-wind equations, and longitudinally

varying solutions that are time independent in a framework corotating with the sun. For the spherically-symmetric cases, we set $\frac{\partial}{\partial\phi} = 0$ in eqs. 6-12; whereas for the corotating case the time derivative in inertial space is replaced by $-\Omega \frac{\partial}{\partial\phi}$, where Ω is the solar angular velocity. Inner boundary conditions are then specified at r = 0.2 AU as a function of t or ϕ, and the MHD equations are integrated numerically outward to 6.0 AU. The longitudinal boundary conditions are periodic in ϕ; the time-dependent boundary condition is chosen to be periodic so that an analogous computation is possible.

For the spherically-symmetric model, eq. 7 is simply the statement that $r^2 B_r$ is conserved, but eq. 8 must be integrated numerically. For the corotating model eq. 7 must be integrated numerically, but it is possible to avoid integrating eq. 8 by choosing an initial condition in which fluid velocity and magnetic field are aligned. Thus, eq. 12 requires that

$$\frac{\partial}{\partial\phi}\left[B_\phi V_r + (\Omega r - V_\phi) B_r\right] = 0 \qquad (18)$$

in the corotating case; we actually determine B_ϕ at the inner boundary by the relation

$$B_\phi = \frac{V_\phi - \Omega r}{V_r} B_r \qquad (19)$$

after other variables have been specified. As the electric field is curl-free, eq. 19 is satisfied everywhere (not just on the inner boundary), and is a conserved quantity.

To facilitate the numerical calculation, we adopt a change of variables;

$$\chi = \phi + \frac{\Omega r}{V_o}, \quad \text{or} \quad \chi = -\Omega t + \frac{\Omega r}{V_o} \tag{20a,b}$$

where V_o is the average solar-wind velocity. The radial variable is not altered and the transformation replaces the original longitudinal variable with a longitudinal variable that remains constant along the average spiral direction. The change of variables introduces additional derivatives with respect to χ on the right hand side of eqs. 6-12 but does not affect the conservation law form. This change of variables allows a larger step size in Δr.

Equations 6-12 can be written in vector form;

$$\frac{\partial \overline{A}}{\partial r} = \frac{\partial \overline{G}}{\partial \chi} + \overline{S} \tag{21}$$

where $\overline{A}$ is a conserved quantity of the flow for those equations for which the $\overline{S}$ component is zero. The numerical calculations are conducted using a predictor-corrector technique. Values of $\overline{A}$ at $r + \Delta r$ are calculated from the right hand side of eq. 21 evaluated at r,

$\overline{A}$ at r, $\overline{A}$ at r - Δr, and a finite difference operator. The difference operator is an adjustable combination of a second-order accurate difference operator and a small contribution from a first-order accurate difference operator chosen to provide numerical dissipation by averaging $\overline{A}$ in the χ direction. The plasma parameters at r + Δr are calculated from $\overline{A}$ and the auxiliary equations by a rapidly convergent iterative technique. The value at r + Δr is then corrected by use of eq. 21 with derivatives and source terms evaluated at r + Δr.

The calculation used a variable step size, Δr, restricted to satisfy the Courant condition (Fox, 1962). In addition, a limit $\Delta r \leq 0.02r$ was imposed; in practice this condition determined the step size. In the χ variable 128 steps were used and the period of repetition was chosen to be 1/3 of a solar rotation for both corotating and spherically symmetric solutions. The stability and accuracy of the solutions were investigated using a variety of different step sizes in the r and χ variables and by altering the amount of numerical dissipation. For the calculations to be described there are no significant errors in the average properties of the flow parameters; further decreases in step size only improve resolution in the vicinity of shocks that form in the flow.

To determine the effects of solar-wind stream structure upon the average properties of the solar wind, we have performed calculations using a variety of inner boundary conditions (both realistic

and unrealistic) to aid in understanding what effects are important in causing the radial gradients that occur in the solution. The results we discuss in this paper are based on the following set of inner boundary conditions imposed at 0.2 AU:

$$V_r = 450 + 150\ (\cos 3\phi), \qquad \text{(km/sec)} \tag{22a}$$

$$V_r = 450 + 200\ (\cos 3\phi) \qquad \text{(km/sec)} \tag{22b}$$

$$V_\phi = 40 \qquad \text{(km/sec)} \tag{23}$$

$$n = 175, \quad n = 175\ (1 - \tfrac{1}{2} \cos 3\phi), \qquad (n/cm^{-3}) \tag{24a,b}$$

$$n = 175\ (1 - .65 \cos 3\phi) \tag{24c}$$

$$T_e = T_i = 3.3\times10^5 \qquad (°K) \tag{25}$$

$$B_r = 100, \quad B_r = 100\ (1 - \tfrac{1}{2} \cos 3\phi), \qquad (\gamma) \tag{26a,b}$$

$$B_r = 125 \tag{26c}$$

Throughout the paper we will discuss primarily calculations using eqs. 22a, 23, 24b, 25, 26a as inner boundary conditions (Case 1); to determine what happens in the absence of density-velocity correlations we substitute 24a for 24b (Case 2); to consider large anticorrelations we use 22b, 23, 24c, 25, 26c (Case 3); and in the section on azimuthal magnetic fields we also use 26b (rather than 26a), 22a, 23, 24b, and 25 (Case 4). These choices are summarized in Table 1, where the entries refer to equation numbers.

A polytrope index of 1.2 is chosen for the electron gas and 5/3 for the ion gas (the proton polytrope index affects only the relation between internal energy and pressure because the proton temperature is determined by the energy conservation equation).

Note that our procedure is different from that of some other workers (e.g., MHD model of Steinolfson et al. (1975)) who specify conditions for all r at t = 0 and then integrate forward in time. We specify a cyclic boundary condition for all time at r = 0.2 AU and then integrate outward in radial distance. At larger distances the evolution of our solutions is similar to that shown in Fig. 2 of Hundhausen and Gosling (1976); the velocity gradients in regions between overtaking streams steepen, forward and reverse shocks form on either side of the compression region, etc. The averages which we report in the following sections are obtained by integrating the solar wind parameters for such solutions over a periodicity cycle, at a fixed radial distance.

Table 1

Inner Boundary Conditions

	V_r	V_ϕ	n	T	B_r
Case 1	22a	23	24b	25	26a
Case 2	22a	23	24a	25	26a
Case 3	22b	23	24c	25	26c
Case 4	22a	23	24b	25	26b

3. DENSITY-VELOCITY CORRELATIONS AND RADIAL GRADIENTS OF PLASMA PROPERTIES

A salient feature of the solar wind which was first noted by Neugebauer and Snyder (1966), and by numerous workers since that time, is the existence of high-speed streams in the solar wind and an anticorrelation between radial velocity and density. As high-speed streams overtake low speed plasma, a compression region develops along the interface between high and low-speed streams. In the case of a source region that rotates with the solar corona, this interface will lie along the average spiral direction of the interplanetary magnetic field. (In the case of a spherically symmetric time-dependent model compression will occur in a spherical shell.)

To consider how such an interaction might evolve with distance, we have integrated the MHD equations of motion for periodic inner boundary conditions at 0.2 AU (Case 1, previous section) with a density and velocity anticorrelation; for the purposes of comparison we have also investigated conditions (Case 2) with high speed streams but with an initially uniform density distribution, and conditions (Case 3) with a larger than average stream structure and associated density-velocity anticorrelation. The numerical calculations were done for both spherically symmetric-time dependent models and time-independent, corotating, azimuthally varying models. The value of radial velocity, averaged over a periodicity cycle (time or longitude), is shown in Fig. 1 as a function of radial distance.

It can be seen that the effects of velocity-density correlations are much greater than the differences between symmetric and corotating models. The predicted decrease in velocity with radial distance is due simply to conservation of momentum; if a high speed, low density object collides with a low speed, high density object, the low density object will be more greatly decelerated than the high density object is accelerated. This is a non-negligible effect; conversion of internal energy and heat conduction energy into kinetic energy at large radial distances would lead to an expected increase of radial velocity of about 25 km/sec between 1 and 6 AU, but actual decreases of 7 to 25 km/sec are calculated. The difference of about 30 to 50 km/sec is due to the non-linear effects of the solar wind density-velocity correlation upon the equations for average solar-wind flow.

The consequences of this decrease in averaged V_r with increasing radial distance for the radial gradient of solar-wind density can be determined by averaging eq. 6 (flux conservation) over a periodicity cycle (longitude or time). We then obtain

$$C = r^2\langle nV_r\rangle = r^2(\langle n\rangle\langle V_r\rangle + \langle \delta n \delta V_r\rangle) \ , \qquad (27)$$

where δ denotes difference of a variable from its average value, brackets denote an average value over longitude (or time), and C is a

constant. We have plotted $r^2\langle n\rangle\langle V_r\rangle$ and $r^2\langle \delta n \delta V_r\rangle$ in Fig. 2 for a spherically symmetric integration of the Case 1 boundary conditions. The anticorrelation between V_r and n decreases with increasing radial distance, and in fact density and velocity are positively correlated at distances greater than 500 solar radii. This rather surprising result arises from a rebound phenomenon; if a high speed, low density stream collides elastically with a low speed, high density stream, the velocity of each stream will simply be reversed in the framework moving with the center of mass. Thus, density and velocity will be positively correlated in the compression region between forward and reverse corotating shocks that form in the solar wind; at large radial distances these regions expand so that most, and eventually all, of the solar wind has been shocked. The consequences of this phenomena for radial gradients of density are significant; the increase in the $r^2\langle \delta n \delta V_r\rangle$ term implies a corresponding decrease in $r^2\langle n\rangle$ with radial distance (6% from 1 AU to 6 AU) despite the fact that V_r is approximately constant. Thus, a steeper than $1/r^2$ fall off of $\langle n\rangle$ need not be interpreted as evidence for a meridionally diverging flow.

To further elucidate the importance of fluctuations we have plotted in Fig. 3 the terms that contribute to radial gradients of radial momentum flux for the same calculation (spherically symmetric Case 1). (Radial momentum flux can not be written in strict conservation law form in a spherical geometry due to geometric source terms.)

Contributions to gradients of $\langle n \rangle \langle V_r \rangle^2$ at distances of 40 to 160 solar radii from both pressure and nonlinear fluctuations are significant; at distances greater than 160 solar radii the fluctuation term dominates. In fact, a decrease of about 15% in the quantity $r^2 \langle n \rangle \langle V_r \rangle^2$ occurs beyond 160 solar radii, while the actual momentum flux carried by the bulk flow undergoes a very slight increase with distance. Thus, a decrease of solar-wind velocity with increasing heliocentric distance must be interpreted with caution. Stream-stream interactions and the resultant correlation between δn and δV_r can explain a velocity decrease without necessarily requiring energy or momentum sinks such as pickup of interstellar neutrals or acceleration of energetic particles.

We have also computed the radial variation of kinetic energy flux (not shown, but dominated by fluctuations similar to Fig. 3); a minimum value of this quantity $r^2 \langle n V_r^3/2 \rangle$ occurs at a model dependent distance of 430 solar radii. At this distance the kinetic energy flux initially present in the form of stream kinetic energy (fluctuations) has been converted into internal energy of the flow (gas and magnetic). At greater radial distances the flow expands, the energy is reconverted into a kinetic flux, and the proportion of energy flux in the bulk flow increases. This interaction is reflected in the radial variation of gas and magnetic pressure (Fig. 3) where local maxima of values integrated over a spherical shell (scaled by r^2) occur at distances of 440 solar radii.

An upper limit for the effect of stream-stream interactions upon the heating of protons can also be estimated. Ion-temperature

gradients might be due to either of two separate effects: adiabatic temperature variations due to compression and expansion of the plasma, and dissipative heating due to corotating shocks. The extent of dissipative heating will depend upon the relative proportions of energy at shocks that is taken up by the electron component of the gas. The effects of electron heat conduction (see Section 2) are approximated in the case of a polytrope law by an increased internal energy (eq. 16) for a given temperature. In addition, the macroscopic flow characteristics such as distance of shock formation and amount of compression should also depend upon radial gradients of electron temperature (and hence polytrope index). Given that some assumptions concerning an electron heat law are made, the proton temperature can then be computed using conservation of energy flux (eqs. 11, 16).

Proton temperature profiles for electron polytrope indexes of 1.2, 1.5, and 5/3 for Case 1 inner boundary conditions with spherical symmetry are shown in Fig. 4. Surprisingly, there is very little difference between the temperatures predicted for electron polytrope indexes from 1.2 to 5/3. We have also plotted the electron-temperature gradient for the case $\gamma_e = 5/3$. As our model puts all dissipative heating in protons, the temperature profile shown represents solely the effects of adiabatic heating by compression. It is apparent that the effects of plasma-density variations upon average values of adiabatically determined temperatures are negligible; the gradient follows closely the $r^{-4/3}$ power law that would be expected for a model without temporal (or longitudinal) variations.

Although our treatment of the electron heat conduction problem is far from ideal, the wide range of electron polytrope indices used should bracket reasonable models for the behavior of the electron gas. Our calculations show a significant minimum in the solar wind proton temperature at 300 solar radii; in the actual solar wind this minimum will be more spread out due to the variable length scales of actual solar wind streams and may not occur at all. A broad plateau with temperatures on the order of 8×10^{4}°K at distances of from 3 to 6 AU is a feature that should be readily apparent in solar wind data. However, this is not guaranteed. For the case of electron polytropic index $\gamma_e = 1.2$, the internal energy (longitudinal average of ρ^{γ_e}) will not be greatly affected by longitudinal density gradients. For $\gamma_e = 5/3$, a substantial percentage increase in the internal energy of the electron gas may occur. However, electron temperatures at 1 AU and beyond are unrealistically low due to the inner boundary condition assumed (it is not possible to model accurately temperature with a polytrope law over a wide range of radial distances). Thus, more energy may be absorbed by adiabatic compression of an electron gas than indicated by the calculations. In addition, dissipative heating of the electron gas as well as the ion gas is to be expected. The ion temperature profiles calculated, although they might be realistic, are best interpreted as plausible upper limits on heating due to stream-stream interactions. A broad

plateau with temperatures on the order of 8×10^4°K at distances of from 3-6 AU is suggested, and may be apparent in the solar wind. An important point to note is that the large decrease in the standard deviation of V_r with increasing radial distance does not imply counter balancing increases in thermal speed. As discussed earlier, transfer between terms in the energy flux equation is much less than might be expected from gradients of products of averaged density and velocity.

4. ANGULAR-MOMENTUM TRANSPORT AND AZIMUTHAL VELOCITY

Measurements of the solar-wind azimuthal velocity and angular-momentum flux are reported by Lazarus and Goldstein (1971) from Mariner 5 plasma and magnetic data; Egidi and Signorini (1974) present measurements of azimuthal velocity obtained from HEOS 1 and Explorer 33 spacecraft; Hundhausen et al. (1970) report Vela 3A and 3B measurements; and Egidi et al. (1969) give Explorer 18 results. The concensus of these observations, despite some disagreement, is an average V_ϕ at 1 AU on the order of 7 to 8 km/sec. These measurements are, however, difficult to obtain, and other effects such as variations on periods of months to years (Egidi and Signorini, 1974) may also be occurring. Tangential velocities as large as 8 km/sec are larger than would be expected on theoretical grounds (Weber and Davis, 1967), but theoretical uncertainties (Weber, 1970, 1972) and non-uniform solar-wind expansion (Priest and Pneuman, 1974) are also significant. Further discussion of observational and theoretical problems are provided by Hundhausen (1972) and in Solar Wind (edited by Sonett et al., 1972, pages 261-275).

For the purpose of estimating radial gradients beyond 1 AU, an inner boundary condition of V_ϕ = 40 km/sec is chosen at 0.2 AU; this results in an average V_ϕ of 8 km/sec at 1 AU. Using a radial magnetic field at 0.2 AU that results in a B_ϕ of 4γ at 1 AU, approximately 2/3 of the angular momentum flux at 1 AU is carried by the plasma and 1/3 by the magnetic field; these values are in

approximate agreement with the 3 to 1 ratio observed by Mariner 5 (Lazarus and Goldstein, 1971). As conditions match observations at 1 AU, the predictions for angular-momentum transport and azimuthal velocity at larger radial distances can be directly determined and compared to observations.

Unlike other plasma parameters, radial gradients of azimuthal velocity and angular momentum flux depend sensitively upon whether a spherically symmetric or corotating model is used. The physical basis for this difference is the orientation of the high pressure compression region between low and high speed streams. In the spherically symmetric model this compression region is a spherical shell, while in the corotating situation the high pressure region is aligned along a spiral interface. Thus, in the spherically-symmetric case pressure gradients act only in the radial direction, while in the corotating case pressure forces also deflect low-speed streams in the direction of solar rotation and high-speed streams in the opposite direction. The effects of this difference can be seen in radial gradients of radial velocity (Fig. 1). Recalling that the average radial velocity decreases because low-density, high-speed, regions are more accelerated than high-density solar wind, the reduced radial pressure gradients of the corotating case result in smaller radial accelerations and less decrease in the average radial

velocity with increasing distance. Another effect of the spiral alignment is that high-speed streams are deflected against the direction of solar rotation and low-speed regions are deflected in the direction of solar rotation (Siscoe et al., 1969). A further point that has not been noted in this regard is that the low mass flux (high speed) regions are more greatly deflected than the high mass flux (low speed) regions in the azimuthal direction with a consequent decrease in average azimuthal velocity with increasing radial distance below the value that would be expected for a solar wind without fluctuations. In fact, we shall demonstrate that at large radial distances (900 solar radii or more) the average solar-wind azimuthal velocity can be in a direction opposite to the solar rotation.

We investigate the effects of density-radial velocity correlations upon azimuthal velocity gradients by integrating models with and without such correlations (Case 1 and Case 2) for spherically symmetric and corotating models (see Fig. 5). The calculations are started at 0.2 AU with rV_ϕ of 8 AU km/sec. For models with no magnetic field or no non-linear fluctuations this quantity would be constant with radial distance if pressure goes to zero sufficiently fast as $r \to \infty$. Weber and Davis (1967) have shown that the effect of including magnetic fields in a spherically-symmetric model results in a transfer of angular momentum from the magnetic field to the plasma with increasing radial distances to yield slight increases in $r\langle V_\phi \rangle$ with distance. In the calculations

we show there is a slight decrease in $r\langle V_\phi \rangle$ between 40 and 70 solar radii; we attribute this to the fact that our solutions do not match properly through the Alfvenic and sonic transition points from a flow that originates in the corona. The decrease near the inner boundary therefore corresponds to damping of inward propagating Alfven waves closer to the sun. From 70 to 425 solar radii there is an increase of about 20% in $r\langle V_\phi \rangle$ for the solutions shown; this modest increase does not occur in our models unless we include both the effects of magnetic fields and solar wind stream structure. The increase is not due to a transfer of angular momentum from the field to the plasma, as our later discussion will show. A similar small increase in the average value of $r\langle V_\phi \rangle$ between the corona and 1 AU was demonstrated in an MHD model that included stream-stream interactions (Urch, 1972).

At larger radial distances (where reexpansion of the compressed plasma dominates) a much larger decrease in the average value of $r\langle V_\phi \rangle$ is predicted. This decrease is due to the deflection of low density, high speed streams in a direction counter to solar rotation. High density plasma ahead of the spiral compression region is accelerated in the corotating direction, but as the density is higher while the pressure forces are equal, the acceleration is less. Consequently, a net decrease in the value of $r\langle V_\phi \rangle$ with distance occurs without necessarily altering the proportion of angular momentum carried by the plasma.

Surprisingly, a similar phenomenon can occur in spherically-symmetric flows. In Fig. 5, the spherically-symmetric calculation with a density-velocity anticorrelation (Case 1) also shows a decrease in $r\langle V_\phi \rangle$ with radial distance, although the gradient is only about half as steep as in the corotating case. The decrease may be attributed to magnetic forces; the bending of field lines in the vicinity of a compression region will tend to accelerate fast plasma counter to the solar rotation direction and slow plasma in the solar rotation direction. As in the corotating case, the density difference between the two streams results in greater acceleration of the high-speed stream with a consequent decrease in the average value of rV_ϕ with radial distance.

An interesting question suggested by these results is whether or not the stream-stream interactions also cause a transfer of angular momentum flux between the magnetic field and the plasma. This question is answered by the results shown in Figs. 6 and 7. The average plasma angular-momentum flux, normalized with respect to an expected r^{-3} dependence, $(r/AU)^3\langle nV_rV_\phi \rangle$ (protons/m sec^2) is plotted as a heavy solid line; brackets denote averages over longitude or time. The angular-momentum flux carried by the magnetic field, $-(r/AU)^3\langle B_rB_\phi \rangle/\mu_o m_p$, is plotted as a thin solid line; the angular momentum fluxes due to fluctuations, $-(r/AU)^3(\langle nV_rV_\phi \rangle - \langle n \rangle \langle V_r \rangle \langle V_\phi \rangle)$, and $(r/AU)^3(-\langle B_rB_\phi \rangle + \langle B_r \rangle \langle B_\phi \rangle)/\mu_o m_p$, are shown as heavy and thin dashed lines. For the case of the spherically-symmetric model this latter quantity is identically zero as B_r cannot vary with time.

Interpretation of the spherically-symmetric solution (Fig. 6) is straightforward. No significant transfer of angular momentum between the plasma and magnetic field occurs at large radial distances; this is in agreement with the conclusions of Weber and Davis (1967). The differences between the angular momentum flux carried by the plasma and the estimate that might be obtained by multiplying appropriate average values of density, radial velocity, and azimuthal velocity together are significant. A comparison of the average value of rV_ϕ with radial distance (Fig. 5) to the difference between averages of products and product of averages (dashed heavy line of Fig. 6) demonstrates that the difference can be attributed directly to correlations between rV_ϕ and r^2V_r that develop as a result of compressions in the solar wind.

The angular-momentum flux for the corotating calculations is shown in Fig. 7. This case is significantly different in that a large transfer of angular momentum from the plasma to the magnetic field occurs as radial distance increases from 200 to 600 solar radii. This can be readily explained by the compression of the magnetic field. The thin dashed line indicating momentum flux carried by magnetic fluctuations exactly follows the increase in total angular momentum flux carried by the plasma. This is in agreement with the idea that transfer of angular-momentum flux to the average magnetic field must be quite small; elsewhere in this

study we show that $\langle B_r \rangle$ and $\langle B_\phi \rangle$ do not vary greatly from r^{-2} and r^{-1} power law behavior as a result of stream-stream interactions. However, compression of the magnetic field into the region between corotating streams results in a non-linear increase in the average value of the product $B_r B_\phi$ although the average values of B_r and B_ϕ are not increased. The difference between the corotating calculation and the spherically-symmetric calculation occurs because B_r is not increased by compression in spherically symmetric models. At distances from 400 to 600 solar radii, kinetic compressive forces are approximately balanced by expansive forces due to gas pressure and the magnetic field. At radial distances greater than 600 solar radii the angular-momentum flux carried by the magnetic field begins to decrease. At these distances, the velocity differences across interaction regions have decayed considerably (Collard and Wolfe, 1974; Smith and Wolfe, 1976; Gosling et al., 1976). Thus, the rebounding plasma expands away from the compression region and the maximum values of $\langle r^2 B_r \rangle$ and $\langle r B_\phi \rangle$ thereafter decrease with increasing radial distance.

5. VARIATION OF AVERAGE AZIMUTHAL MAGNETIC FIELD WITH RADIUS

The radial variation of the azimuthal interplanetary magnetic field B_ϕ is a subject of considerable observational and theoretical interest. A number of observations have been reported of the radial variation of the average of B_ϕ (Burlaga and Ness, 1968; Coleman and Rosenburg, 1968; Rosenburg, 1970; Coleman et al., 1969; Rosenburg and Coleman, 1973; Smith, 1974; Villanti and Mariani, 1975; Behannon, 1975). The observations have generally indicated that the average of B_ϕ (averaged over time periods of the order of 27 days) tends to fall off more steeply than the 1/r dependence expected for a constant solar wind. Jokipii (1975, 1976) pointed out that short period fluctuations in the wind velocity could change the radial dependence of averaged solar-wind parameters. In this section we examine the numerical solutions described in section 2 and show that for certain sets of boundary conditions, the effect of fluctuations on $\langle B_\phi \rangle$ can be significant.

Before discussing the numerical calculations, we discuss the expected radial variation of the average B_ϕ in terms of averages and correlations between fluctuations. The evolution of the ϕ component magnetic field is determined by eq. 8.

We suppose that the wind velocity is the superposition of a mean value plus a fluctuating part

$$\overline{V} = \langle \overline{V} \rangle + \delta \overline{V} = \langle V_r \rangle \overline{e}_r + \langle V_\phi \rangle \overline{e}_\phi + \delta \overline{V}$$

Similarly, we set $\overline{B} = \langle\overline{B}\rangle + \delta\overline{B}$. Taking the average over ϕ of eq. 8, the derivative with respect to ϕ drops out, $\langle B_\phi\rangle$ depends only on r, and we can define the variable A_1 by

$$A_1 = \langle V_r\rangle\langle B_\phi\rangle - \langle V_\phi B_r\rangle = \frac{C}{r} - \langle\delta V_r \delta B_\phi\rangle + \langle\delta V_\phi \delta B_r\rangle \qquad (29)$$

eq. 29 is a slight generalization of eq. 5b of Jokipii (1975); C is an arbitrary constant. As $\langle V_r\rangle$, $\langle B_r\rangle$, and $\langle V_\phi\rangle$ can be determined from other equations, $\langle B_\phi\rangle$ can be found from A_1. Note that in the absence of fluctuations, and since $\langle V_\phi\rangle$ is small compared with $\langle V_r\rangle$, one expects that if $\langle V_r\rangle$ is constant, $\langle B_\phi\rangle \propto 1/r$, as in the Archimedean spiral. It is a general consequence of $\nabla\cdot\overline{B} = 0$ that $r^2\langle B_r\rangle$ is a constant, even in the presence of arbitrarily large fluctuations. Thus eq. (29) in the absence of fluctuations corresponds to the conventional spiral magnetic field. Deviations of A_1 from a 1/r dependence imply deviations from the spiral.

The computer-generated solutions were examined to determine the relative importance of the various terms appearing in eq. 29. The average values of $\overline{V}$ and $\overline{B}$ were constructed at each radius by averaging over solar longitude. The correlations of the fluctuations were constructed by computing the difference between the value at each point and the average, and then computing the longitudinal average of the relevant products of the differences. As the numerical integration is done in conservation law form, eq. 29 is exactly satisfied by the solutions obtained and an exact r^{-2} dependence for B_r also results.

We found in our corotating model that with inner boundary conditions including a density-radial velocity anticorrelation and constant magnetic field (Case 1), the left hand side of eq. 29 could be accurately represented by a 1/r dependence; so, the effect of fluctuations was not great. However, without the density-velocity anticorrelation (Case 2), or with an inner-boundary correlation between magnetic field and velocity (Case 4), the effects of the fluctuations were significant. Shown in Fig. 8 is the quantity $A_1 = \langle V_r \rangle \langle B_\phi \rangle - \langle V_\phi \rangle \langle B_r \rangle$ plotted as a function of r for Case 4. For comparison a 1/r curve is also shown. Clearly A_1 departs significantly from a 1/r dependence. A least squares fit to A_1 between 1 and 6 AU gives $A_1(r) = r^{-1.05}$. As the term $\langle \delta B_\phi \delta V_r \rangle$ is much larger than $\langle \delta B_r \delta V_\phi \rangle$, fluctuations act upon B_ϕ to distort the spiral interplanetary magnetic field. To demonstrate this we have evaluated the right side of eq. 29, including the correlation term. The quantity $A_1 + \langle \delta V_r \delta B_\phi \rangle = A_2$ should vary as 1/r, since $\langle \delta V \delta B_r \rangle$ is small. The quantity A_2 has been evaluated in this case and follows the expected 1/r dependence quite well. A least squares fit to A_2 gives a power law dependence of $r^{-1.002}$.

We conclude that with inner boundary conditions corresponding to Cases 2 and 4 the average azimuthal magnetic field can deviate significantly from the Archimedean spiral based on the average radial wind velocity.

DISCUSSION AND SUMMARY

There has already been a good deal of discussion of the role of stream-stream interactions in reducing the amplitude of velocity variations in the solar wind at large radial distances (Collard and Wolfe, 1974; Smith and Wolfe, 1976; Hundhausen and Gosling, 1976; Gosling et al., 1976). In addition, our calculation predicts a modest decrease of the solar wind speed at large radial distances. Collard et al. (1975) have reported a tendency for the solar wind velocity between Pioneer 11 and Pioneer 10 to decrease when velocities at Pioneer 11 are above 450 km/sec; in addition, a decrease between Pioneer 11 and Pioneer 10 of the average velocity of about 30 km/sec occurs (Wolfe, personal communication). Our model calculations predict a decrease from 1 to 6 AU on the order of 7 to 25 km/sec, as opposed to the 25 km/sec increase that would be expected from conversion of thermal and magnetic energy into kinetic energy in models without fluctuations. The magnitude of the deceleration that we predict depends obviously upon the magnitude of initial density-velocity anticorrelation assumed at 0.2 AU, but is also crucially dependent on the assumed magnetic field strength, density, and pressure at distances of 200 to 600 AU; reexpansion of the compressed plasma is enhanced for higher Alfven and sonic speeds. This expansion results in a positive correlation between density and radial velocity in the solar wind if only the region between forward and

reverse corotating shocks is considered. At large radial distances this region expands sufficiently so that there is a net positive correlation in the solar wind as a whole; a resultant decrease in both the average radial velocity and r^2n at increasing distances occurs as a result of the increasing correlation. The decrease in amplitude of radial velocity fluctuations does not imply large increases in proton temperature as considerable adiabatic compression can occur while actually decreasing the average solar-wind temperature; an estimate based on a crude treatment of the electron thermal properties suggests a plateau between 3 to 6 AU with maximum average ion temperatures on the order of 8×10^{4}°K.

We have also demonstrated the rather surprising conclusion that at large radial distances the average solar-wind azimuthal velocity may be in a direction opposed to the solar rotation. Assuming a solar-wind tangential velocity of 8.5 km/sec at 1 AU, values of 2.5 km/sec at 4 AU and 1.2 km/sec at 6 AU would be expected in the absence of stream-stream interactions. In fact, our calculations show that the same mechanism that reduces the radial solar-wind velocity also results in azimuthal velocities of 0.25 km/sec at 4 AU and -1.7 km/sec at 6 AU (Fig. 5) in corotating models; for spherically-symmetric models, a velocity of +0.2 km/sec at 6 AU is expected. The total difference at 6 AU due to density-velocity anticorrelation is between 1 to 3 km/sec which corresponds to angular deviations of from 0.1 to 0.4°. Measuring such relative changes in angle between 1 and 6 AU is well within the capabilites of present plasma experiments; if care is taken in determining

detector and spacecraft alignments, an absolute measurement of the counterrotation should also be possible. Continuous coverage, however, is an important requirement for such studies, as large variations of V_ϕ occur due to stream interaction regions, Alfven waves, and other sources of variation.

We have also predicted that the major fraction of angular-momentum flux will be carried by magnetic fluctuations (large scale MHD fast waves after Schubert and Coleman, 1968) at distances on the order of 3 to 4 AU. This effect should also be observable, despite some controversy that has recently been attached to an apparent $r^{-1.3}$ dependence of the azimuthal magnetic field. Parker and Jokipii (1976) have recently demonstrated that variations in $\langle V_r \rangle$ can account for the anomalous radial gradient observed on Pioneer 10; the same correction should be made for B_ϕ when computing radial gradients of angular momentum flux. An additional problem that impacts estimates of radial gradients of field components is correcting for the reverse in direction due to sector structure (Rosenberg et al., 1975); as angular-momentum flux depends only upon the product of B_r and B_ϕ this problem will not influence observations of momentum flux. Determinations of radial gradients in angular-momentum flux, like other solar-wind properties, can best be made by comparison between data obtained simultaneously from two spacecraft at different radial distances; otherwise temporal variations (e.g., solar-cycle velocity variations) might bias the observations.

Average magnetic field components are also affected by stream interactions; if a correlation between B_r and V_r at the inner boundary is assumed, a 10% decrease in $\langle rB_\phi \rangle$ between 1 and 6 AU occurs. However, such a correlation is not especially large in the solar wind (Goldstein and Siscoe, 1972); several other models tested without an initial correlation showed decrease in $\langle rB_\phi \rangle$ of between 0 and 10%.

In summary, nonlinear fluctuations are a significant effect in determining the radial gradients of the solar wind at distances as small as 0.2 AU; at distances greater than 1 AU nonlinear fluctuations dominate the behavior of the radial gradients. Therefore, it would be desirable that future studies of solar wind gradients should directly average conserved quantities (left hand side of eqs. 6-12), as well as the usual parameters such as magnetic field, density, velocity, temperature, and so on. Such averages will allow direct estimates of the importance of nonlinear fluctuations in determining radial gradients, and are essential for investigating effects that are ignored by conventional MHD models, such as energy or momentum loss to nonthermal particles or newly ionized solar wind neutrals.

ACKNOWLEDGMENTS

We are grateful to E. J. Smith and M. Neugebauer for a helpful review of this manuscript. The portion of this work conducted at the Jet Propulsion Laboratory of the California Institue of Technology is one phase of research supported by NASA under contract NAS 7-100. JRJ acknowledges the support of the National Aeronautics and Space Administration under Grant NSG-7101.

FIGURE CAPTIONS

Figure 1. The radial dependence of the average value of V_r with an initial density-velocity anticorrelation (Case 1, thick lines) and without an initial correlation (Case 2, thin lines). Spherically-symmetric calculations for Cases 1 and 2 are shown as solid lines, corotating calculations as dashed lines. A spherically-symmetric calculation for a large density-velocity anticorrelation (Case 3) is shown as alternating long and short dashes.

Figure 2. The radial dependence of solar-wind number density and the product of density and velocity. The long-short dashed line is the product of average density multiplied by r^2 and the average product of average density multiplied by r^2 and the average velocity. The short dashed line is the difference between the number density flux, a conserved quantity, and the product just described.

Figure 3. Terms entering the radial momentum flux equation, all quantities have been divided by the proton mass and multiplied by r^2.

Figure 4. The ion temperature as a function of radial distance. The short-long dashed curve is the electron temperature that results from adiabatic changes ($\gamma_e = 5/3$). The (solid, dotted, dashed) line represents the ion temperature that results if a polytrope law for the electron gas is used with index of (1.2, 1.5, 5/3).

Figure 5. The radial dependence of the average value of rV_ϕ with an initial density-velocity anticorrelation (Case 1, thick lines) and without an initial correlation (Case 2, thin lines). Spherically-symmetric calculations are shown as solid lines and corotating calculations as dashed lines.

Figure 6. Angular-momentum flux for the spherically symmetric model with an initial density-velocity anticorrelation (Case 1). The heavy solid line is the quantity $r^3\langle nV_r V\rangle$; the heavy dashed line is the quantity $r^3(\langle nV_r V_\phi\rangle - \langle n\rangle\langle V_r\rangle\langle V_\phi\rangle)$. The thin solid line is the quantity $-r^3\langle B_r B_\phi\rangle/\mu_0 m_p$; the thin dashed line is $-r^3(\langle B_r B_\phi\rangle - \langle B_r\rangle\langle B_\phi\rangle)/\mu_0 m_p$. Units are $AU^3(protons/m^3)(m/sec)^2$.

Figure 7. Angular-momentum flux for the corotating model; variables shown as for Figure 6.

Figure 8. The radial dependence of the quantity $(\langle V_r\rangle\langle B_\phi\rangle - \langle V_\phi\rangle\langle B_r\rangle) = A_1$ for a corotating calculation with an initial correlation between magnetic field and radial velocity assumed (Case 4). A 1/r power law is shown as a solid line, while the best fit power law dependence of $1/r^{1.05}$ between 1 and 6 AU is shown as a dashed line. The dots are points from the numerical solution. Units are gamma × m/sec.

REFERENCES

Behannon, Kenneth W., Variation of the Interplanetary Magnetic Field with Heliocentric Distance, Preprint #X-692-75-143, Goddard Space Flight Center, Greenbelt, Md.

Burlaga, L. F., and N. F. Ness, Macro- and Micro-structure of the Interplanetary Magnetic Fields, Can. J. Phys., 46, 5962, 1968.

Coleman, P. J., Jr., and R. L. Rosenberg, The Radial Dependence of the Interplanetary Magnetic Field: 1.0-0.7 AU (Abstract), Trans. Amer. Geophys. Union, 49, 727, 1968.

Coleman, Paul, Jr., Edward J. Smith, Leverett Davis, Jr., and Douglas E. Jones, The Radial Dependence of the Interplanetary Magnetic Field: 1.0-1.5 AU, J. Geophys. Res., 74, 2826, 1969.

Collard, H. R., and J. H. Wolfe, Radial Gradient of Solar Wind Velocity from 1 to 5 AU, in SOLAR WIND THREE, edited by C. T. Russell, 281, Inst. of Geophysics and Planetary Physics, U. of Calif., Los Angeles, 1974.

Collard, H. R., J. D. Mihalov, and J. H. Wolfe, Radial Gradient of Solar Wind Velocity from 1 to 7 AU (Abstract), EOS, 56, 1055, 1975.

Edigi, A., G. Pizella, and C. Signorini, Measurement of the Solar Wind Direction with IMP 1 Satellite, J. Geophys. Res., 74, 2807, 1969.

Egidi, A., and C. Signorini, Solar Wind Direction from HEOS 1 and Explorer 33 Satellites, Solar Phys., 34, 247, 1974.

Fox, L., Numerical Solution of Ordinary and Partial Differential Equations, p. 205-229, Addison-Wesley, Reading, Mass., 1962.

Goldstein, B. E., and G. L. Siscoe, Spectra and Cross Spectra of Solar Wind Parameters from Mariner 5, in SOLAR WIND, 506, edited by C. P. Sonett, P. J. Coleman, and J. M. Wilcox, NASA Sp-308, 1972.

Gosling, J. T., A. J. Hundhausen, and S. J. Bame, Solar Wind Stream Evolution at Large Heliocentric Distances: Experimental Demonstration and the Test of a Model, J. Geophys. Res. (in press), 1976.

Hundhausen, A. J., S. J. Bame, J. R. Asbridge, and S. J. Sydoriak, Solar Wind Proton Properties: Vela 3 Observations from July 1965 to June 1967, J. Geophys. Res., 75, 4643, 1970.

Hundhausen, A. J., Solar Wind and Coronal Expansion, Springer-Verlag, New York, 84-90, 1972.

Hundhausen, A. J. and J. T. Gosling, Solar Wind Structure at Large Heliocentric Distances: An Interpretation of Pioneer 10 Observations, J. Geophys. Res., 81, 1436, 1976.

Jokipii, J. R., Fluctuations and the Radial Variation of the Interplanetary Magnetic Field, Geophys. Res. Let., 2, 473, 1975.

Jokipii, J. R., Radial Variation of Solar-Wind Parameters, Geophys. Res. Let., 3, 141, 1976.

Lazarus, A. J., and B. E. Goldstein, Observations of the Angular Momentum Flux Carried by the Solar Wind, Astrophys. J., 168, 1971.

Nerney, S. F., and S. T. Suess, Corrections to the Azimuthal Component of the Interplanetary Magnetic Field Due to Meridional Flow in the Solar Wind, Astrophys. J., 200, 503, 1975.

Neugebauer, M., and C. W. Snyder, Mariner 2 Observations of the Solar Wind, 1, Average Properties, J. Geophys. Res., 71, 4469, 1966.

Neugebauer, M., The Quiet Solar Wind, J. Geophys. Res., accepted for publication, 1976.

Parker, G. D., and J. R. Jokipii, The Spiral Structure of the Interplanetary Magnetic Field, submitted to Geophys. Res. Let., 1976.

Pizzo, V., J. T. Gosling, A. J. Hundhausen, and S. J. Bame, Large-Scale Dynamical Effects upon the Solar Wind Flow Parameters, J. Geophys. Res., 78, 6469, 1973.

Priest, E. R., and G. W. Pneuman, The Influence of Non-Uniform Solar Wind Expansion on the Angular Momentum Loss from the Sun, Solar Physics, 34, 231, 1974.

Rhodes, E. J., Jr., and E. J. Smith, Multispacecraft Study of the Solar Wind Velocity at Interplanetary Boundaries, J. Geophys. Res., 80, 917, 1975.

Rosenberg, R. L., and P. J. Coleman, Jr., The Radial Dependence of the Interplanetary Magnetic Field: 1.0-0.7 AU, Inst. Geophys. and Planet. Phys. Publ. No. 1196-26, U. of Calif., Los Angeles, 1973.

Rosenberg, R. L., M. G. Kivelson, S. C. Chang, and E. J. Smith, The Radial Dependence of the Interplanetary Magnetic Field Between 1.0 and 5.0 AU: Pioneer 10, Publ. 1500, Inst. Geophys. and Planet. Phys., Univ. of Calif., Los Angeles, 1975.

Rossi, B., and S. Olbert, Introduction to the Physics of Space, 273-306, McGraw-Hill Book Co., New York, 1970.

Schubert, G., and P. J. Coleman, Jr., The Angular Momentum of the Solar Wind, Astrophys. J., 153, 943, 1968.

Siscoe, G. L., The Solar Wind Problem with Fluctuations, Cosmic Electrodyn., 1, 51, 1970.

Siscoe, G. L., B. E. Goldstein, and A. J. Lazarus, An East-West Asymmetry in the Solar Wind Velocity, J. Geophys. Res., 74, 1159, 1969.

Smith, E. J., Radial Gradients in the Interplanetary Magnetic Field Between 1.0 and 4.3 AU: Pioneer 10, p. 257, SOLAR WIND THREE, edited by C. T. Russell, Inst. of Geophys. and Planetary Phys., U. of Calif., Los Angeles, 1974.

Smith, E. J., and J. H. Wolfe, Observations of Interaction Regions and Corotating Shocks Between One and Five AU: Pioneers 10 and 11, Geophys. Res. Let., 3, 137, 1976.

Sonett, C. P., P. J. Coleman, and J. M. Wilcox (editors), SOLAR WIND, NASA SP-308, articles and discussion pp. 261-275, 1972.

Suess, S. T., A. J. Hundhausen, and V. Pizzo, Latitude-Dependent Nonlinear Solar-Wind Streams, J. Geophys. Res., 80, 2023, 1975.

Suess, S. T., and S. F. Nerney, Meridional Flow and the Validity of the Two-Dimensional Approximation in Stellar-Wind Modeling, Astrophys. J., 184, 17, 1973.

Steinolfson, R. S., M. Dryer, and Y. Nakagawa, Numerical MHD Simulation of Interplanetary Shock Pairs, J. Geophys. Res., 80, 1223, 1975.

Urch, I. H., Azimuthal Structure in the Solar Wind, Cosmic Electrodynamics, 3, 316, 1972.

Villanti, U., and F. Mariani, On the Radial Variation of the Interplanetary Magnetic Field: Pioneer 6, Geophys. Res. Let., 2, 73, 1975.

Weber, E. J., and L. Davis, Jr., The Angular Momentum of the Solar Wind, Astrophys. J., 148, 217, 1967.

Weber, E. J., The Torque on the Interplanetary Plasma due to its Anisotropy, Solar Phys., 13, 240, 1970.

Weber, E. J., Comments in SOLAR WIND, 268-271, edited by Sonett et al. (see ref.), 1972.

Winge, C. R., Jr., and P. J. Coleman, Jr., First Order Latitude Effects in the Solar Wind, Planet. Space Sci., 22, 439, 1974.

PRECEDING PAGE BLANK NOT FILMED

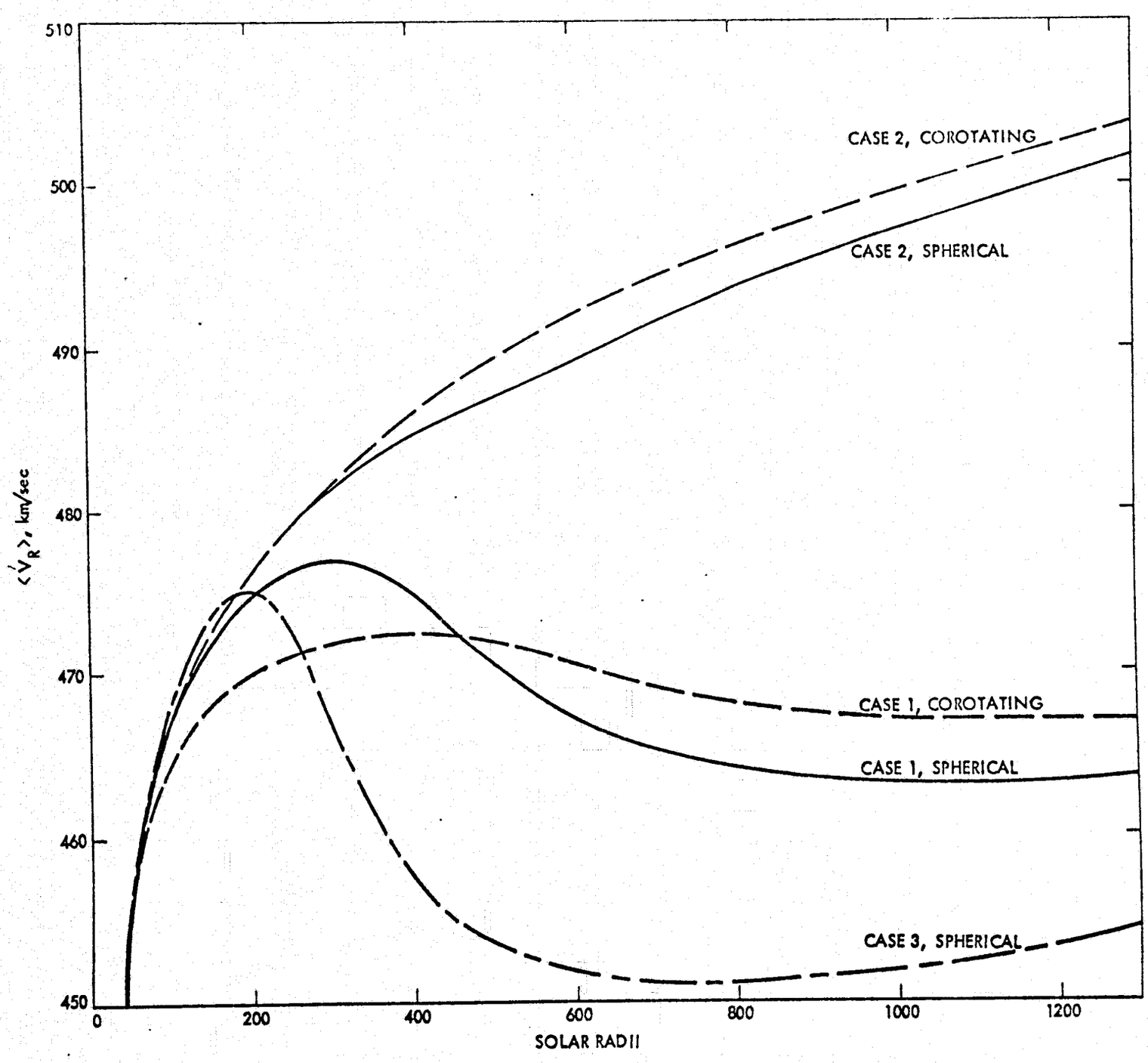

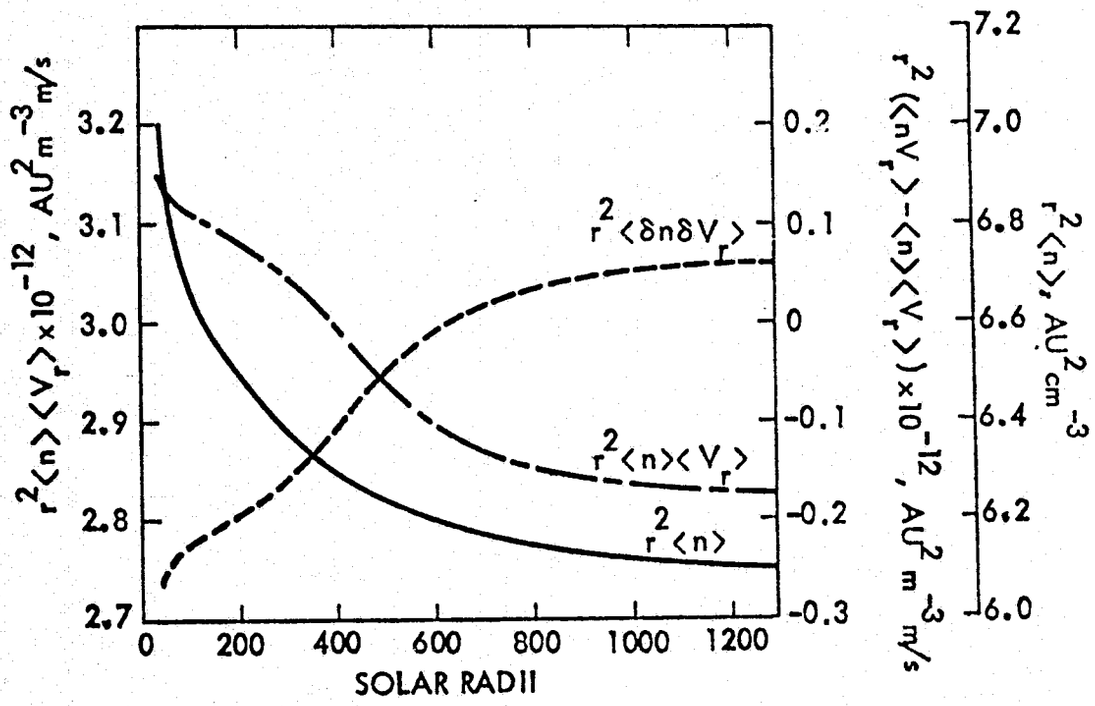
$r^2\langle n\rangle\langle V_r\rangle \times 10^{-12}$, $AU^2 m^{-3} m/s$
$r^2\langle \delta n \delta V_r\rangle$
$r^2\langle n\rangle\langle V_r\rangle$
$r^2\langle n\rangle$
$r^2(\langle nV_r\rangle - \langle n\rangle\langle V_r\rangle) \times 10^{-12}$, $AU^2 m^{-3} m/s$
$r^2\langle n\rangle$, $AU^2 cm^{-3}$
3.2
3.1
3.0
2.9
2.8
2.7
0.2
0.1
0
-0.1
-0.2
-0.3
7.2
7.0
6.8
6.6
6.4
6.2
6.0
0
200
400
600
800
1000
1200
SOLAR RADII

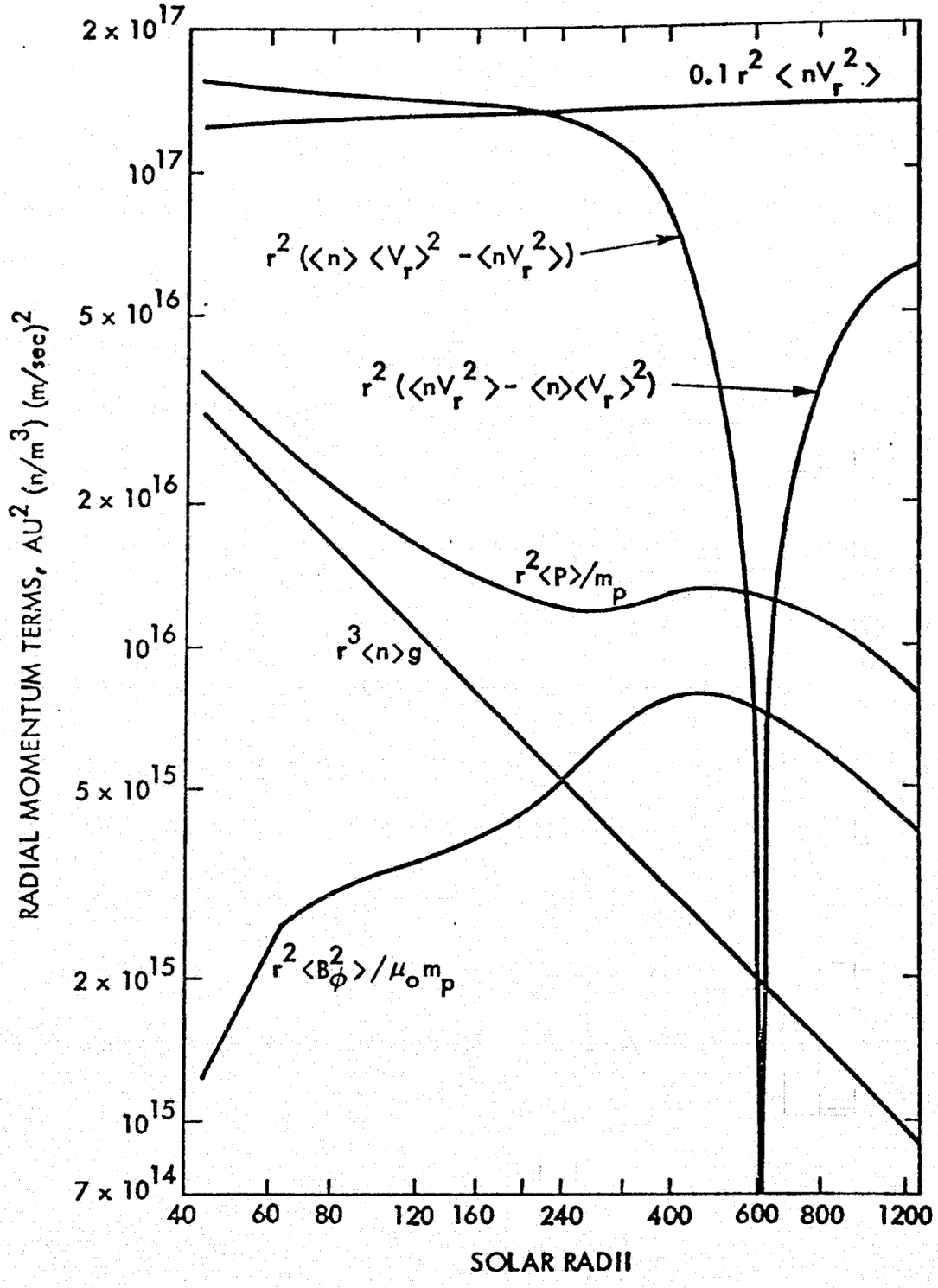
2×10^{17}
10^{17}
5×10^{16}
2×10^{16}
10^{16}
5×10^{15}
2×10^{15}
10^{15}
7×10^{14}
$0.1\, r^2 \langle nV_r^2 \rangle$
$r^2 (\langle n \rangle \langle V_r \rangle^2 - \langle nV_r^2 \rangle)$
$r^2 (\langle nV_r^2 \rangle - \langle n \rangle \langle V_r \rangle^2)$
$r^2 \langle P \rangle / m_p$
$r^3 \langle n \rangle g$
$r^2 \langle B_\phi^2 \rangle / \mu_o m_p$
RADIAL MOMENTUM TERMS, $AU^2\ (n/m^3)\ (m/sec)^2$
40
60
80
120
160
240
400
600
800
1200
SOLAR RADII

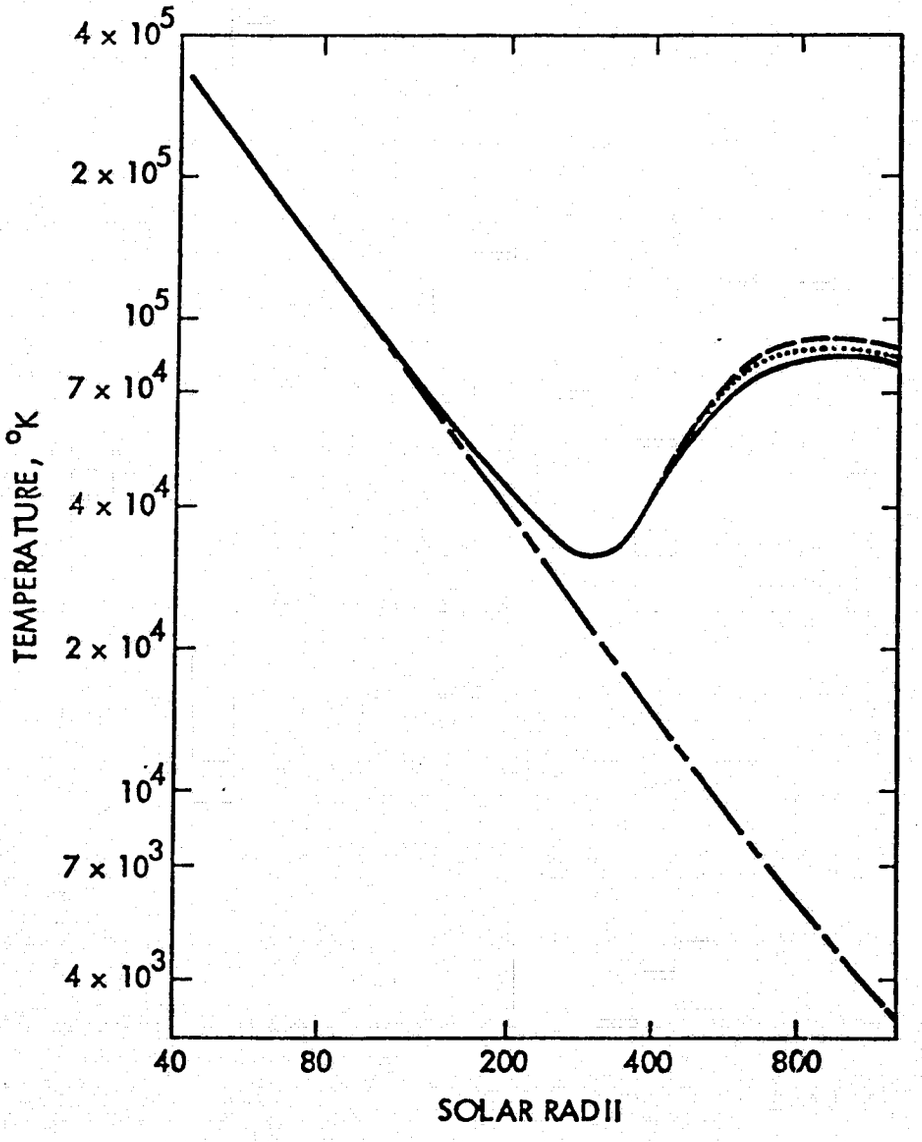
4 × 10^5
2 × 10^5
10^5
7 × 10^4
4 × 10^4
2 × 10^4
10^4
7 × 10^3
4 × 10^3
TEMPERATURE, °K
40
80
200
400
800
SOLAR RADII

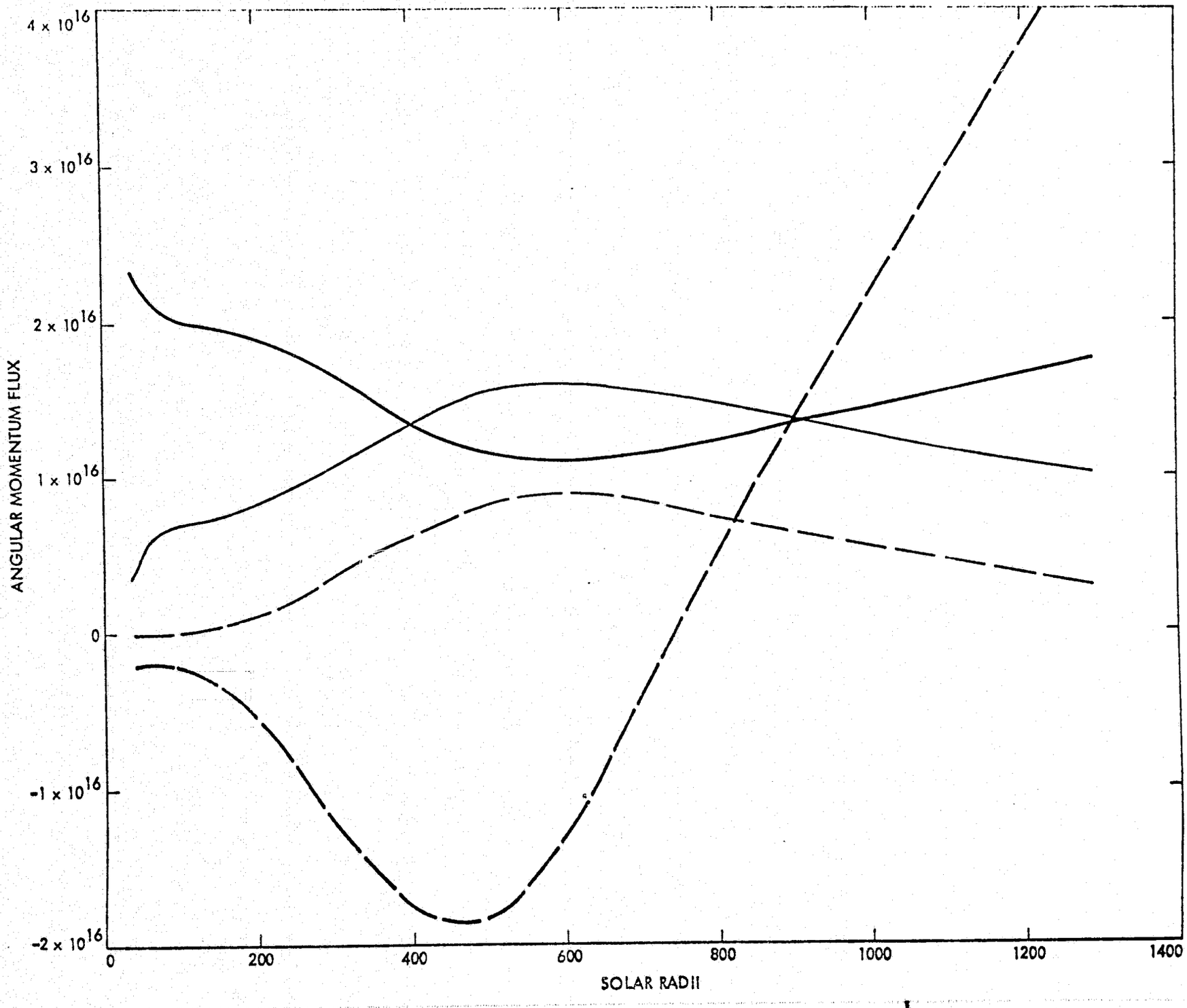
4 x 10^16
3 x 10^16
2 x 10^16
1 x 10^16
0
-1 x 10^16
-2 x 10^16
ANGULAR MOMENTUM FLUX
0
200
400
600
800
1000
1200
1400
SOLAR RADII

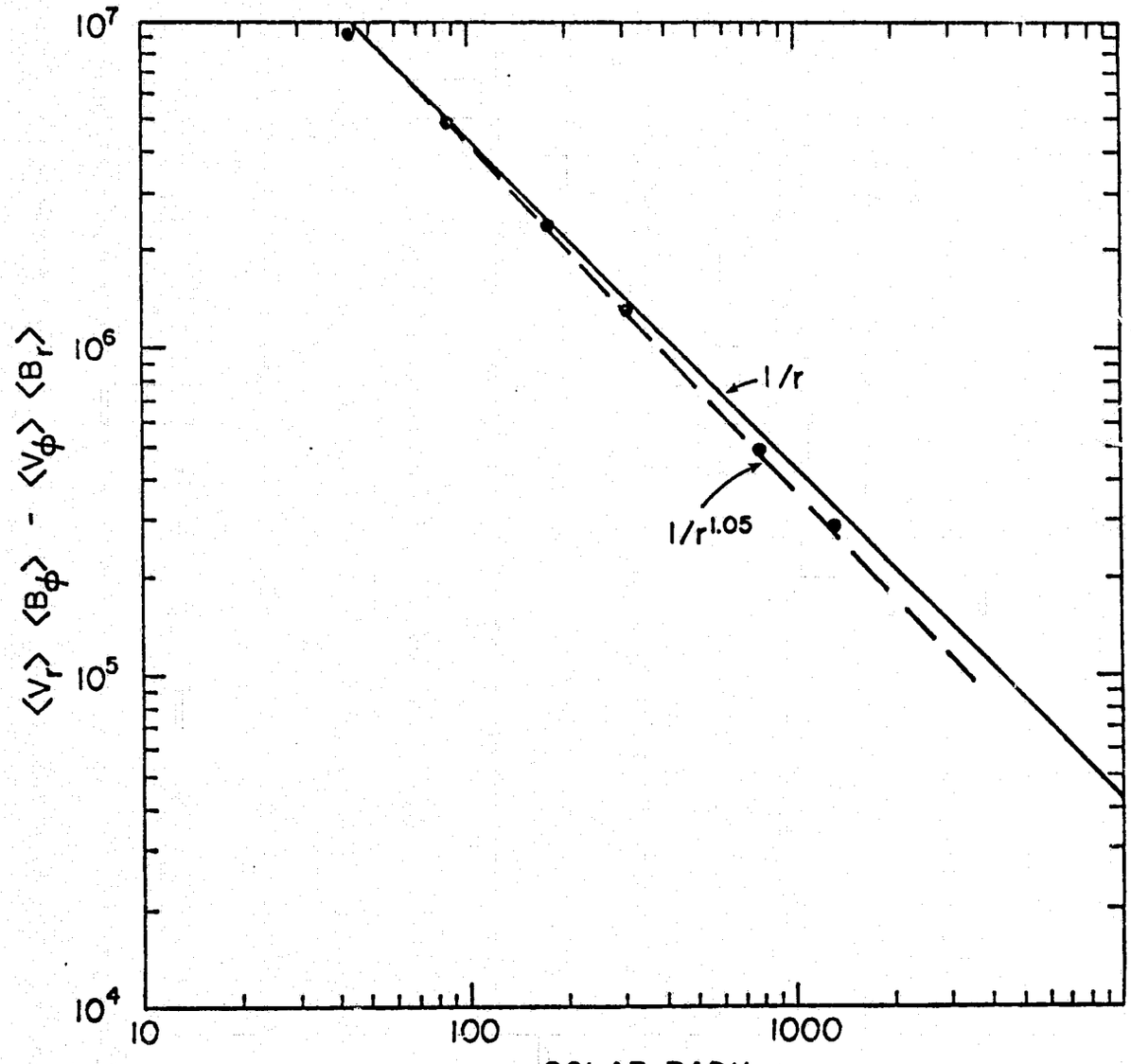
10^7
10^6
10^5
10^4
10
100
1000
SOLAR RADII
$\langle V_r \rangle \langle B_\phi \rangle - \langle V_\phi \rangle \langle B_r \rangle$
1/r
$1/r^{1.05}$

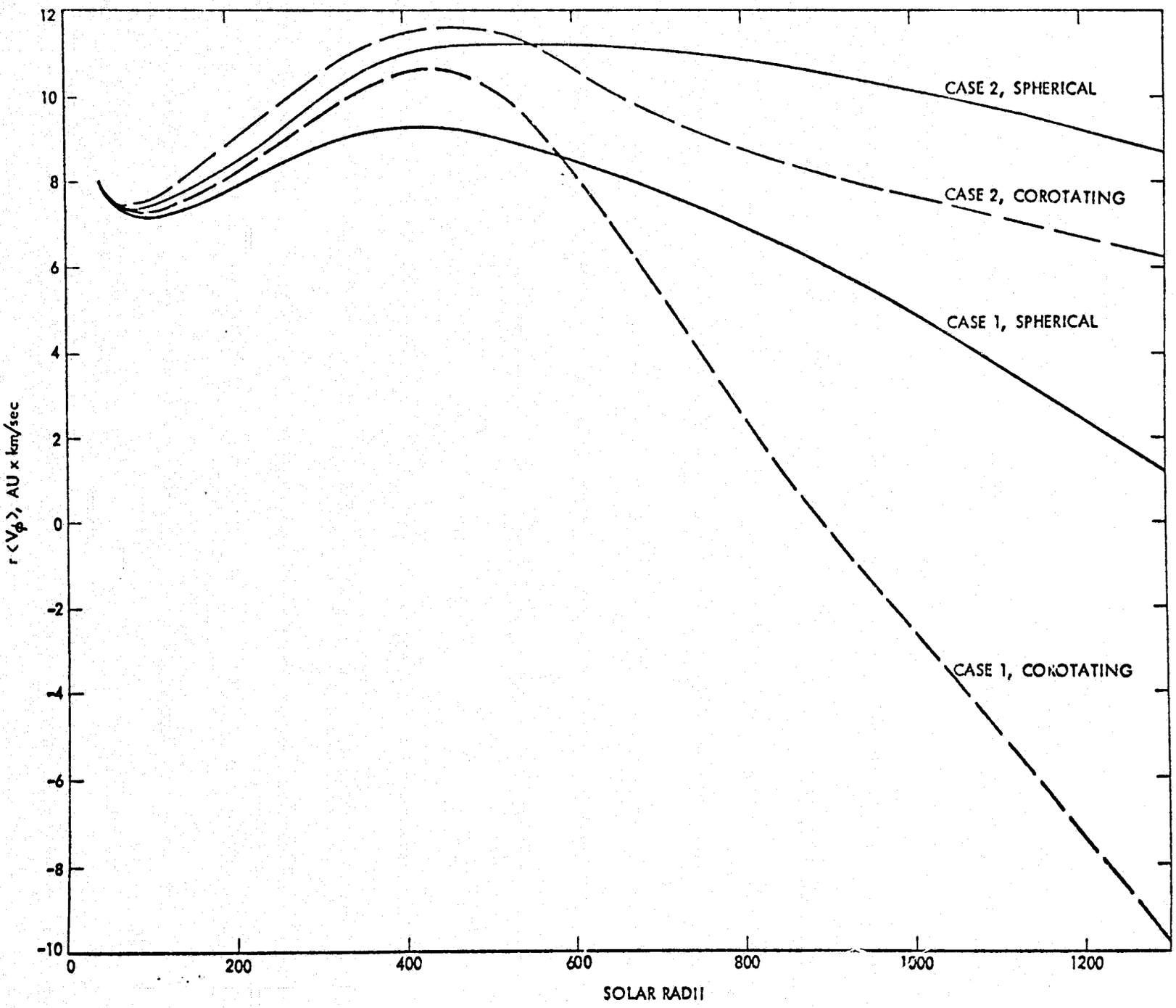
12
10
8
6
4
2
0
-2
-4
-6
-8
-10
0
200
400
600
800
1000
1200
SOLAR RADII
r <Vφ>, AU x km/sec
CASE 2, SPHERICAL
CASE 2, COROTATING
CASE 1, SPHERICAL
CASE 1, COROTATING

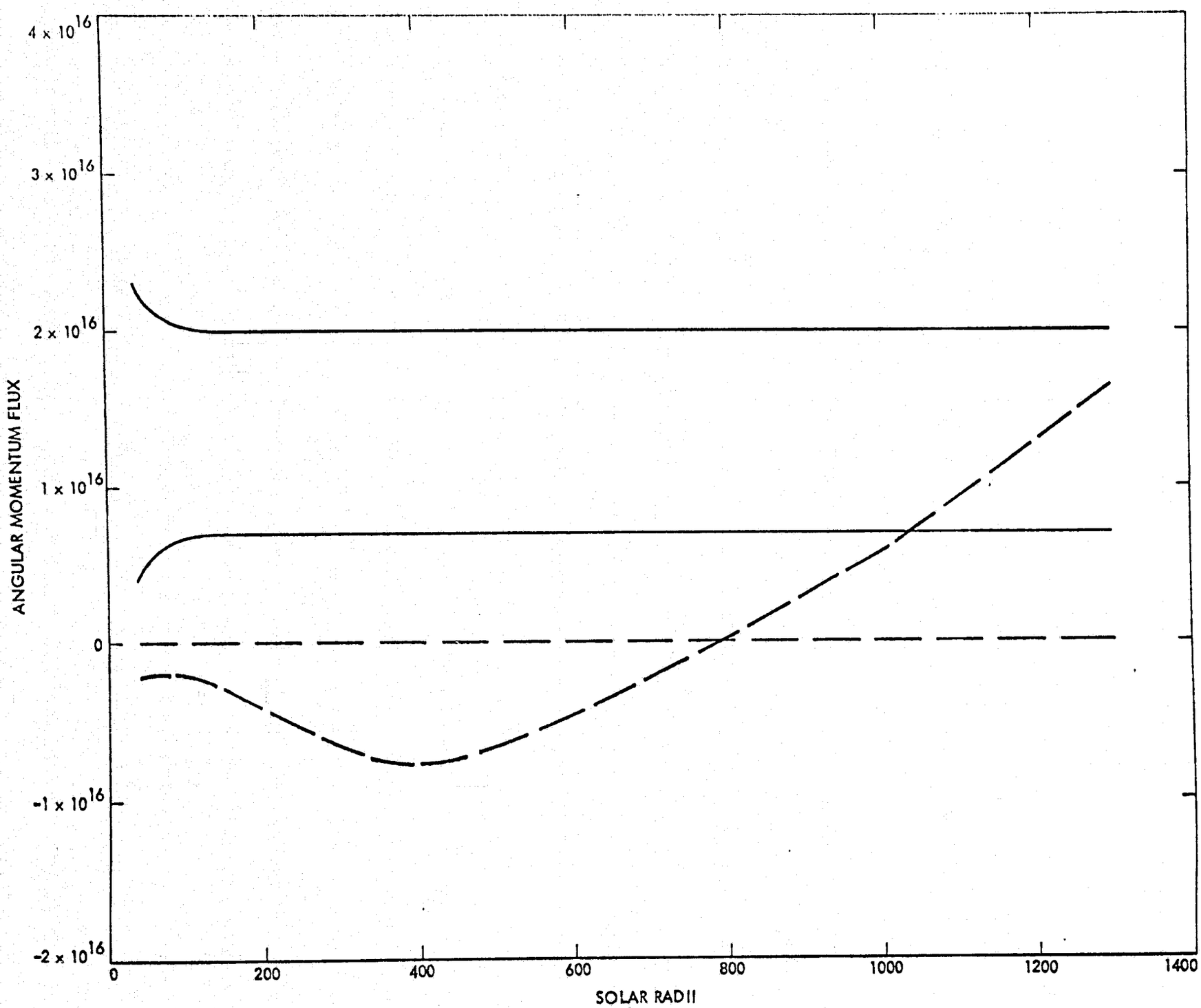
4 x 10^16
3 x 10^16
2 x 10^16
1 x 10^16
0
-1 x 10^16
-2 x 10^16
ANGULAR MOMENTUM FLUX
0
200
400
600
800
1000
1200
1400
SOLAR RADII